

Beyond Reward: A Bounded Measure of Agent–Environment Coupling

Wael Hafez
Semarx Research LLC
Alexandria, VA, USA.
w.hafez@semarx.com

Cameron Reid
Semarx Research LLC
Alexandria, VA, USA
Cameron.reid@semarx.com

Amer Nazeri
Semarx Research LLC
Alexandria, VA, USA
Amir.nazeri@semarx.com

Abstract— Real-world reinforcement learning (RL) agents operate in closed-loop systems where actions shape future observations, making reliable deployment under distribution shifts a persistent challenge. Existing monitoring relies on reward or task metrics, capturing outcomes but missing early coupling failures. We introduce bi-predictability (P) as the ratio of shared information in the observation–action–outcome loop to the total available information — a principled, real-time measure of interaction effectiveness with provable bounds, comparable across tasks. An auxiliary monitor, the Information Digital Twin (IDT), computes P and its diagnostic components from the interaction stream. We evaluate SAC and PPO agents on MuJoCo HalfCheetah under eight agent- and environment-side perturbations across 168 trials. Under nominal operation, agents exhibit $P = 0.33 \pm 0.02$, below the classical bound of 0.5, revealing an informational cost of action selection. The IDT detects 89.3% of perturbations versus 44.0% for reward-based monitoring, with $4.4 \times$ lower median latency. Bi-predictability enables early detection of interaction degradation before performance drops and provides a prerequisite signal for closed-loop self-regulation in deployed RL systems.

Keywords— Reinforcement learning, deployment monitoring, information theory, digital twin, agent-environment coupling, anomaly detection

I. INTRODUCTION

A. RL deployment as closed-loop

Deep reinforcement learning (RL) has achieved strong results in continuous control and robotics, with growing real-world deployment [1], [2], [3]. Deployed RL agents operate in closed-loop systems, where observations guide actions that shape future observations [4]. In practice, this interaction can be disrupted by environmental shifts, sensor degradation, or actuator drift, often degrading performance before overt failure is observed [5], [6].

B. Reward-Based Monitoring is Reactive and Incomplete

Current deployment monitoring typically relies on episodic reward signals, return-based evaluation, or input distribution tracking to assess agent health [7], [8], [9]. When degradation is detected, the response is reactive: offline retraining on newly

collected trajectories, manual intervention, or threshold-based alarms that trigger fallback behaviors [6], [10].

C. No Real-Time Signals Monitors the Full Interaction Loop

Coupling degradation often goes unnoticed until performance collapses, leading to costly retraining or manual intervention. What is missing is a real-time, task-independent early warning signal that monitors the full interaction loop. Existing methods track only inputs or outcomes, detect failures only after substantial performance loss, and rely on task-specific rewards that lack a cross-task baseline. Related approaches such as Active Inference [11], [12] and Empowerment [13], [14] quantify one-way influence rather than the bidirectional coupling required for robust agency. This motivates the need for a task-independent metric to compare interaction quality across agents and deployment settings.

D. Bi-Predictability Addresses These Limitations

We show that bi-predictability (P)—the ratio of shared information in the observation–action–outcome loop to the total available information—addresses key limitations of existing monitoring by analyzing the full interaction in real time and providing a task-independent reference with an upper bound of 0.5. We introduce the Information Digital Twin (IDT), which computes P and its diagnostic components online from the (S, A, S') stream and uses their union as a multi-channel detector.

Unlike traditional digital twins that replicate physical states [15], [16], the IDT monitors the informational integrity of agent–environment coupling, detecting degradation across diverse perturbations with higher coverage and lower latency than reward-based methods. This establishes a prerequisite signal for closed-loop self-regulation under changing deployment conditions.

We evaluate the framework on SAC and PPO agents, in MuJoCo HalfCheetah-v4 with frozen policies. Eight agent- and environment-side perturbations are applied across 21 seeds, yielding 168 trials. P and its components are computed over sliding windows without access to internal models or rewards, and detection coverage, latency, and diagnostic specificity are

benchmarked against reward-based monitoring. Trained agents exhibit a stable baseline of $P \approx 0.33$, confirming that active control incurs an inherent trade-off between predictive coherence and agentic freedom.

E. Contributions

We make the following contributions¹:

1. We validate bi-predictability (P) as a real-time, task-independent measure of RL agent–environment coupling integrity in continuous control.
2. We demonstrate that IDT-based monitoring detects 89.3% of perturbations compared with 44.0% for reward-based detection, with $4.4 \times$ lower median latency.
3. We show that the diagnostic decomposition provides complementary detection channels — the union achieves higher coverage and lower latency than any individual metric, revealing a rich diagnostic profile that enables future attribution analysis.
4. We present the IDT architecture as a lightweight, deployable monitoring module that operates without access to internal model parameters or reward signals, establishing a prerequisite for closed-loop self-regulation.

II. RELATED WORK

A. RL Deployment Robustness and Monitoring

RL robustness research has primarily focused on preventative strategies — domain randomization, adversarial training, and robust policy optimization — to mitigate the sim-to-real gap [5]. These methods improve policy resilience at training time but do not monitor interaction integrity during deployment. Post-deployment monitoring typically relies on input distribution tracking [7], [8] or episodic return evaluation [6], both of which detect degradation reactively and only after substantial performance loss. Non-invasive, task-independent monitoring of the full observation–action–outcome loop — the gap identified in *I.C* — remains unaddressed by these approaches.

B. Information-Theoretic Measures in RL

Information theory offers a principled way to quantify agent–environment interactions. Empowerment captures an agent's capacity to influence future states [11], [13], [14], and Active Inference views agent behavior as minimizing variational free energy for stability [12]. However, these measures focus on unidirectional influence—either the agent's control over the environment or vice versa—rather than the bidirectional dynamics of the full interaction loop.

Our prior work demonstrated that the mutual information shared across the observation–action–outcome loop, $MI(S, A; S')$, detects behavioral anomalies in robotic control [17]. Bi-predictability (P) builds on this by normalizing for total information and adding regime-dependent bounds, allowing

direct comparison of interaction quality across agents, tasks, and deployment settings.

C. Digital Twins in Robotics

Digital twins (DTs) have progressed from static CAD models to real-time, synchronized virtual replicas that are essential in industry for predictive maintenance, condition monitoring, and operational assurance [15], [16]. In robotics, DTs help ensure safety, track actuator degradation, and enable virtual commissioning to reduce deployment risk. With growing system complexity, extending DTs to monitor both physical states and decision-making health is increasingly important.

III. BI-PREDICTABILITY FRAMEWORK

A. Information-Theoretic Preliminaries

Entropy $H(S)$ quantifies the uncertainty, or unpredictability, of a random variable — the larger its value, the less predictable the variable's realizations. Mutual information $MI(S, A; S')$ then measures how much knowing one set of variables reduces uncertainty about another: specifically, how much the joint observation–action pair (S, A) shares informationally with the outcome S' [18], Fig. 1.

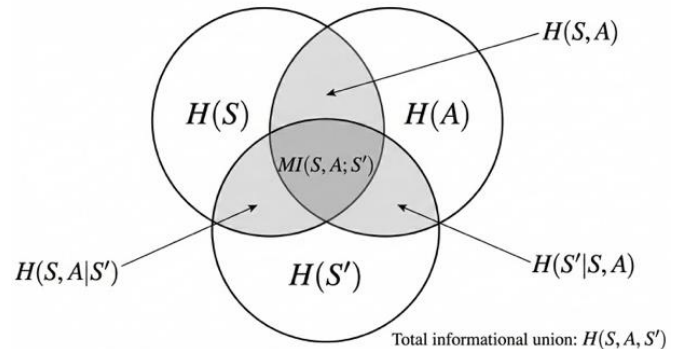


Fig. 1. Information-theoretic structure of the observation–action–outcome interaction. Each circle represents the entropy of one variable: observations $H(S)$, actions $H(A)$, and outcomes $H(S')$. The central overlap is the mutual information $MI(S, A; S')$; non-overlapping regions correspond to conditional entropies. *Note on visual representation:* While the central overlap is labeled $MI(S, A; S')$ for clarity, it serves as a visual proxy for the joint mutual information; mathematically, $MI(S, A; S')$ corresponds to the entire region of S' shared with the (S, A) union. Bi-predictability (P) is defined as the ratio of this shared information to the total informational union $H(S, A, S')$.

Conditional entropy quantifies the uncertainty remaining in one variable after another is known. For example, $H(S'|S, A)$ is the uncertainty in the outcome after both the observation and action are known; in Fig. 1 this corresponds to the region of the S' circle that falls outside its overlap with (S, A) . Conversely, $H(S, A|S')$ is the uncertainty remaining in the observation–action pair after observing the outcome. These quantities decompose total uncertainty into shared and unshared parts: $H(S') = MI(S, A; S') + H(S'|S, A)$. That is, the outcome's total uncertainty equals the information it shares with the observation–action pair plus what remains unexplained [19].

¹ Github repository: https://github.com/Semarxai/idt_app

The interaction cycle poses the predictive question at the heart of deployment monitoring: given an observation and action, what is the next outcome? We focus on how much the state–action pair (S, A) , treated jointly, shares with the outcome S' — that is, $MI(S, A; S')$ (Fig. 1). When $MI(S, A; S')$ is high relative to the total uncertainty across all three variables, the interaction loop is tightly coupled: the agent and environment are highly predictable to one another. When it is low, the loop is informationally loose — outcomes are poorly predicted by the agent's state and actions, or the agent's behavior is poorly reflected in what follows.

B. Bi-Predictability: Definition and Classical Bound

Building on the information-theoretic quantities introduced above, we define bi-predictability P as the ratio of shared information to the total informational budget of the interaction cycle:

$$P = \frac{MI(S, A; S')}{H(S) + H(A) + H(S')} \quad (1)$$

The denominator $C = H(S) + H(A) + H(S')$ is the total entropy capacity deployed across the observation–action–outcome loop. P therefore measures the fraction of this budget that is common to both sides of the interaction — not the volume of information exchanged, but the efficiency with which the loop's informational resources support mutual predictability.

At the extremes, $P = 0$ indicates that the observation–action pair and the outcome are statistically independent — knowing one side tells nothing about the other. The upper bound, derived below, represents the case where each side fully specifies the other.

To establish this bound, we note that mutual information cannot exceed the entropy of either side of the interaction: $MI(S, A; S') \leq H(S, A)$ and $MI(S, A; S') \leq H(S')$. Since the joint entropy is itself bounded by the sum of marginals, $H(S, A) \leq H(S) + H(A)$, it follows that:

$$MI(S, A; S') \leq \min(H(S) + H(A), H(S')) \quad (2)$$

Under the fixed budget constraint $H(S) + H(A) + H(S') = C$, the function $\min(H(S) + H(A), H(S'))$ subject to $H(S) + H(A) + H(S') = C$ is maximized when $H(S) + H(A) = H(S') = C/2$. Therefore, the maximum achievable value of the numerator is $C/2$, yielding:

$$P \leq \frac{1}{2} \quad (3)$$

This bound is structural, arising directly from Shannon entropy and holding for any classical system representable by these variables, independent of domain, task, or agent architecture. The full derivation and saturation conditions are given in [24]; here we summarize the result relevant to deployment monitoring.

C. What Determines Bi-Predictability

Detecting deviations in agent–environment coupling is necessary for monitoring, but understanding their cause is essential for effective intervention. Responses differ, for example, when degradation arises from environmental unpredictability versus indistinguishable agent actions. To enable this distinction, we analyze the internal structure of P within its classical bound. P approaches its maximum of $1/2$ when the shared information $I(S, A; S')$ reaches $C/2$, requiring conditional entropies to vanish in both directions—so outcomes are fully determined by observation–action pairs and these pairs are recoverable from outcomes. In real RL deployments, these conditions are not met, making it critical to identify what limits P from reaching its bound.

Two quantities provide the answer. Forward predictive uncertainty measures how much the outcome remains uncertain after the observation and action are known:

$$H_f = H(S' | S, A) \quad (4)$$

Backward predictive uncertainty measures how much the observation–action pair remains uncertain after the outcome is observed:

$$H_b = H(S, A | S') \quad (5)$$

These are the two sources of informational "leakage" in the interaction loop. When H_f is high, the agent's observations and actions fail to constrain what happens next — the environment responds in ways the agent cannot anticipate. When H_b is high, many distinct observation–action pairs lead to the same outcome — the agent's internal distinctions are invisible from the environment's side.

Their difference defines the predictive asymmetry:

$$\Delta H = H_f - H_b \quad (6)$$

A passive physical system without actions shows balanced uncertainties ($\Delta H \approx 0$), as seen in double-pendulum experiments [24]. When actions are introduced, this balance is disrupted: the agent's interventions cause $|\Delta H| > 0$, with the sign of ΔH revealing whether predictive failures originate from the environment (ΔH positive) or the agent (ΔH negative). P and ΔH together clarify interaction dynamics: P assesses overall coupling, while ΔH shows the source of influence. Section IV explains how the Information Digital Twin computes these values in real time, and Section VI demonstrates that different perturbations yield distinct component signatures.

D. Calculating Information Metrics from Continuous Interactions

The entropies, mutual information, and conditional entropies that define P and ΔH assume discrete probability distributions. For continuous interaction streams, we therefore discretize variables into bins and accumulate transitions over sliding windows of length W with stride δ . Within each window, empirical joint and marginal frequencies of the discretized (S, A, S') tuples are used to compute all information-theoretic

quantities. This yields a time-indexed sequence of P and ΔH values that tracks coupling integrity during deployment. The choice of bin resolution, window length, and stride trades off estimation fidelity against temporal responsiveness; the specific parameters used here are reported in Section V.

IV. REAL-TIME MONITORING OF BI-PREDICTABILITY

Section III showed that P captures the shared information structure of the interaction loop, while its components H_f , H_b and ΔH localize predictive failures. To serve as a deployment monitoring signal, these quantities must be computed online from the interaction stream, without access to internal model parameters or reward signals. We introduce the Information Digital Twin (IDT) (Fig. 2), an auxiliary architecture that runs alongside the deployed agent and computes P and its components directly from the (S, A, S') stream.

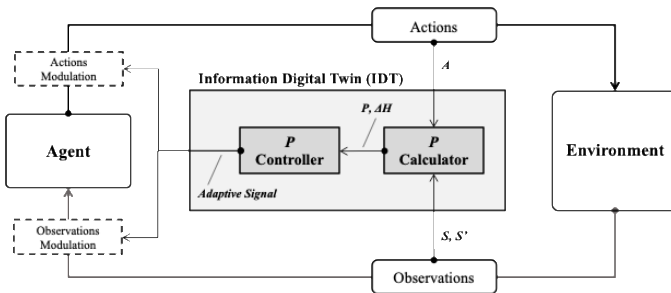


Fig. 2. Information Digital Twin (IDT) architecture. The IDT operates alongside the agent–environment loop, receiving copies of observations (S, S') and actions (A). The P Calculator calculates bi-predictability P and predictive asymmetry ΔH from the interaction stream. The P Controller detects statistical deviations from baseline coupling. Dashed boxes indicate architecturally specified modulation pathways — observation modulation and action modulation — that are not experimentally validated in this work. The Adaptive Signal path connects controller output to the modulation interfaces.

The IDT operates in three stages: online metric estimation (IV-A), statistical detection of deviations from the learned baseline (IV-B), and a modulation stage—architecturally specified but not yet experimentally validated—that would adapt the agent’s observation and action interfaces in response to sustained deviations (IV-C).

A. Calculating P from the Interaction Stream

The IDT treats the deployed agent as a black box: it observes only the externally visible interaction stream and requires no access to policy weights, internal activations, or reward signals. At each time step, the agent selects an action A given its current observation S , the environment transitions, and a new observation S' is produced. The IDT intercepts copies of this (S, A, S') tuple and estimates P and its diagnostic components through the following pipeline:

1. Capture. Record each (S, A, S') transition tuple from the live interaction stream.
2. Discretize. Map the continuous-valued variables into discrete representations suitable for entropy estimation.
3. Window. Accumulate tuples over a sliding window of fixed length to construct empirical joint and marginal

frequency distributions.

4. Compute. Calculate the marginal entropies $H(S), H(A), H(S')$, the joint mutual information $MI(S, A; S')$, and the conditional entropies $H_f = H(S'|S, A)$ and $H_b = H(S, A|S')$ from the windowed distributions.
5. Derive. Obtain $P = MI(S, A; S') / [H(S) + H(A) + H(S')]$ and $\Delta H = H_f - H_b$ for the current window.

Steps 2 through 5 repeat at each window stride, producing a time series of P and ΔH values that track coupling integrity as the agent operates. The pipeline itself is general: it applies to any system expressible as an (S, A, S') interaction loop, with the estimation fidelity governed by the windowing and discretization parameters.

B. Detecting Deviations from Baseline Coupling

The time series produced by the estimation pipeline provides a continuous readout of coupling integrity, but raw values of P and ΔH are not directly interpretable without a reference. The P controller (Fig. 2) establishes this reference during an initial calibration period under nominal operation by estimating the baseline mean μ and standard deviation σ for each metric. Subsequent values are evaluated against this learned baseline using the following protocol:

1. Calibrate. During a pre-perturbation period of stable operation, compute the mean μ and standard deviation σ of $P, \Delta H, H_f$, and H_b across baseline windows.
2. Compare. For each new window, evaluate whether any metric has deviated beyond $\pm 3\sigma$ from its baseline mean.
3. Flag. A detection is registered when any single metric — $P, \Delta H, H_f$, or H_b — exceeds its threshold. The union of all four channels constitutes the IDT detection signal. A detection latency of zero indicates that the first post-perturbation window already exceeds the threshold. Trials in which no metric exceeds the threshold at any point are recorded as undetected.

The pattern of which metrics deviate, and in which direction, carries diagnostic information that differs across perturbation types. These diagnostic signatures are characterized in Section VI-D; operationalizing them as an automated attribution mechanism is future work.

The $\pm 3\sigma$ threshold is used because deviations in either direction indicate issues: in general terms, a decrease in P shows decoherence, while an increase indicates rigidity. Using four metrics improves detection, since different perturbations affect components differently.

C. Toward Reflexive Modulation

The IDT includes two post-detection pathways that modulate the observation and action interfaces (dashed boxes, Fig. 2). Sustained deviations trigger bandwidth adjustments—such as observation filtering or action damping—without altering policy weights, preserving learned behavior while mitigating coupling degradation. Deviations dominated

by H_f target observations, while those dominated by H_b target actions. This work validates detection and diagnostics; modulation mechanisms are specified but not implemented, with control laws left for future work.

V. EXPERIMENTAL SETUP

A. Environment and Agents

We evaluate our framework on MuJoCo HalfCheetah-v4 [20], a continuous-control benchmark with 17-dimensional observations and 6-dimensional torque actions. The task is to maximize forward velocity under control costs. HalfCheetah provides sufficient complexity for nontrivial information-theoretic estimation while remaining interpretable. Agents are trained using Soft Actor-Critic (SAC) [21] and Proximal Policy Optimization (PPO) [22], implemented in Stable-Baselines-3 [23] with default hyperparameters.

This This pairing tests whether bi-predictability monitoring generalizes across policy architectures. SAC agents were trained to convergence ($\approx 10k - 17k$ returns) over $\sim 2M$ steps, while PPO agents converged faster ($\approx 6k - 8k$ returns) over $\sim 1.5M$ steps. Convergence was defined by stable returns over a sustained evaluation window, after which policies were frozen. Using algorithms with different performance levels tests whether P captures interaction structure independent of raw task performance. In total, 11 SAC and 10 PPO seeds were evaluated, yielding 21 agents. Each evaluation comprised 50 episodes (50,000 steps). Freezing policies ensures that all observed P deviations reflect perturbation-induced coupling changes rather than ongoing learning. The perturbation suite is described next.

B. Perturbation Design

To assess generalization across failure modes, we designed a perturbation suite spanning environment-side interaction changes and agent-side observation and action degradations, with type and severity varied to test detection sensitivity. Environment perturbations include gravity changes (one level) and external force impulses (two levels), while agent perturbations include observation noise (two levels) and action noise (three levels). The eight conditions are summarized in Table 1.

TABLE 1. Perturbation suite. Eight perturbation conditions spanning agent-side and environment-side changes applied to all 21 agents for 168 total trials.

Category	Type	Parameter
Agent	Actuator noise	1% Gaussian noise on actions
Agent	Actuator noise	3% Gaussian noise on actions
Agent	Actuator noise	4% Gaussian noise on actions
Environment	External force	5 N force applied to torso, x- axis
Environment	External force	10 N force applied to torso, x-axis
Environment	Gravity	Gravity increased to 110%
Agent	Observation noise	1% Gaussian noise on observations
Agent	Observation noise	3% Gaussian noise on observations

This suite does not exhaust the space of possible perturbations, which is effectively unbounded in continuous control settings. Instead, it samples qualitatively distinct failure mechanisms across multiple severity levels, supporting task-independent sensitivity rather than tuning to specific failure modes. Each perturbation is introduced at episode 15 of a

50-episode evaluation, yielding 14 unperturbed episodes for baseline calibration. All eight perturbation types are applied to each of the 21 agents, for a total of 168 trials. Information metric computation for these trials is described next.

C. Information Metrics Computation and Comparison Protocol

Computing information-theoretic quantities from the HalfCheetah interaction stream requires discretizing 40 continuous variables per timestep (17 state, 6 actions, 17 next-state). We apply a three-step procedure: z-score normalization, discretization into three equal-width bins, and grouping variables by body part (front leg, back leg, torso) following the environment’s kinematic structure. Per-variable bins within each group are concatenated to form composite symbols for (S, A, S') . This grouping preserves embodiment structure while keeping the joint distribution tractable. The three-bin choice was empirically validated: four bins produced unreliable entropy estimates at available window sizes, while quantile-based binning yielded flat, uninformative metrics. P, H_f, H_b , and ΔH are computed over sliding windows of 300 timesteps with a stride of 50, yielding 991 windows per evaluation. All quantities use standard base-2 entropy formulas. For comparison, per-step reward is averaged over identical windows, and the same $\pm 3\sigma$ detection protocol is applied to both IDT metrics and windowed reward, ensuring matched temporal resolution and fair comparison.

VI. RESULTS

A. Trained Agents Exhibit Stable Coupling Below the Classical Bound

Before evaluating detection performance, we characterize the informational baseline of nominal agent–environment interaction. Under unperturbed operation, the 21 trained agents exhibit a mean bi-predictability of $P = 0.33 \pm 0.02$ and a mean predictive asymmetry of $\Delta H = -0.56 \pm 0.22$, stable across the pre-perturbation episodes of all 168 evaluation runs. The baseline $P = 0.33$ lies well below the classical upper bound of 0.5 [24], indicating that roughly one-third of the interaction’s total informational budget is shared. The negative ΔH shows that forward prediction (anticipating S' from S and A) carries greater residual uncertainty than backward inference (recovering S and A from S'), reflecting the asymmetry of active control: committed actions constrain backward inference more strongly than stochastic environmental responses constrain forward prediction. These baselines define the reference for perturbation-induced deviations. Each seed’s baseline mean and standard deviation are used to calibrate the $\pm 3\sigma$ detection protocol.

B. IDT-Based Monitoring Detects Twice the Perturbations That Reward Signals Miss

We evaluate whether monitoring bi-predictability from the interaction stream detects coupling degradation missed by reward-based monitoring. The $\pm 3\sigma$ detection protocol is applied identically to IDT metrics ($P, \Delta H, H_f, H_b$) and windowed episode reward across all 168 perturbation trials.

IDT-based monitoring detected $89.3 \pm 15.1\%$ of perturbations, compared with $44.0 \pm 26.1\%$ for reward-based

detection (paired t-test, $n = 21$ seeds; $t = 7.95$, $p < 10^{-6}$, $d = 1.73$). Detection rates were computed per seed as the proportion of perturbation trials detected and averaged across seeds. The improvement arises from two factors: IDT metrics respond to changes in interaction structure that may not immediately affect cumulative reward, and the union of four diagnostic channels provides broader coverage than a single reward signal. A detection is registered when any metric exceeds its $\pm 3\sigma$ threshold; different perturbations activate different subsets of channels, but collectively they capture most conditions tested. Reward-based monitoring remains effective for perturbations that cause large, sustained performance drops. However, perturbations that degrade coupling without immediate reward collapse (e.g., moderate observation noise partially compensated by the policy) often go undetected by reward while producing clear deviations in P or its components. This “silent degradation” regime motivates the proposed framework.

C. The IDT Detects Coupling Degradation $4.4\times$ Faster Than Reward

Beyond detecting more perturbations, timely detection is critical for deployment monitoring, as early warning enables intervention before irreversible performance degradation. Detection latency is measured as the number of observation windows between perturbation onset (episode 15) and the first window in which any metric exceeds its $\pm 3\sigma$ threshold.

Across all 168 perturbation trials, IDT-based monitoring achieved a median detection latency of 42 windows, compared with 184 windows for reward-based detection—a $4.4\times$ improvement. This gap reflects a fundamental signal difference: PPP responds to structural changes in the interaction at the transition level, whereas reward aggregates effects over episodes and requires degradation to accumulate before deviating. In deployment terms, earlier detection provides a larger window for corrective action, including operator alerts, fallback policies, or—within a future closed-loop architecture—reflexive modulation.

D. The Diagnostic Decomposition Provides Complementary Detection Channels

The IDT’s detection advantage over reward arises from the complementary sensitivity of multiple information-theoretic channels rather than any single metric. Table 2 reports the individual detection rate and median latency for each monitored quantity, their union (IDT), and reward. No single metric dominates: individual detection rates cluster between 69–73%, exceeding reward-based detection (44.0%) but falling well short of the union (89.3%).

TABLE 2. Per-metric detection rate and median latency across 168 perturbation trials. IDT (union) registers detection when any metric exceeds $\pm 3\sigma$. $P =$ bi-predictability; $Hf = H(S'|S, A)$; $Hb = H(S, A|S')$; $\Delta H = Hf - Hb$. Reward uses the same $\pm 3\sigma$ protocol on windowed episodic return.

Metric	Detection Rate (%)	Median Latency (windows)
IDT (union)	89.3	42
P	73.2	74
Hf	70.8	69
Hb	69.6	75
ΔH	69.0	67
Reward	44.0	184

A similar pattern holds for latency, with individual medians between 67–75 windows versus 42 for the union. This gap—approximately 16 percentage points in coverage and 25 windows in latency—demonstrates that each channel detects perturbations missed by the others; the metrics are complementary, not redundant.

This complementarity is further reflected in per-algorithm effect sizes. For SAC agents, information-theoretic metrics are approximately twice as sensitive as reward (mean Cohen’s $d = 0.93 - 1.02$ vs. 0.60), whereas PPO agents exhibit comparable sensitivity across all metrics ($d \approx 0.5$). Nevertheless, the IDT outperforms reward-based detection for both algorithms—through stronger individual signals for SAC and through the union of channels for PPO, where individual metrics alone are insufficient.

These four quantities represent only a subset of the information structure available in the (S, A, S') interaction loop. The full joint distribution supports a broader family of information-theoretic measures—conditional entropies, pairwise and conditional mutual informations, and interaction information—each potentially sensitive to distinct failure modes. Systematically mapping these sensitivities to perturbation types constitutes a formal attribution analysis enabled by this framework but left for future work.

VII. DISCUSSION

A. Summary of Principal Findings

This study examined if the observation–action–outcome loop offers monitoring benefits beyond reward-based methods. Results show: (1) RL agents have a consistent coupling baseline ($P = 0.33 \pm 0.02$), confirming theoretical predictions and providing a task-independent reference for degradation; (2) IDT-based monitoring detects 89.3% of perturbations—far better than reward signals (44.0%)—and does so with much lower latency; (3) breaking down diagnostics into separate channels further improves coverage and speed. Overall, bi-predictability emerges as an effective, real-time signal for monitoring deployed RL systems and supports closed-loop self-regulation.

B. P Monitors Interaction Structure, Not Task Performance

Bi-predictability and reward measure fundamentally different quantities. Reward aggregates task outcomes over episodes, whereas P captures the shared information structure of the observation–action–outcome loop at the transition level. This distinction produces a regime of silent degradation: perturbations that erode coupling without immediate reward collapse. Across 168 trials, reward-based monitoring missed 56% of perturbations, many of which produced clear deviations in P or its components. For example, moderate observation noise (1% Gaussian) was partially compensated by the policy, leaving reward within baseline while P and Hf deviated beyond 3σ —signaling that the agent’s predictive relationship with the environment had degraded despite sustained task performance.

Existing deployment monitoring methods operate in the same signal space as reward. Return-based evaluation [6], out-of-distribution detection [7], [8], and concept drift tracking [9] each capture fragments of the interaction—inputs, outputs, or

accumulated returns — but none measures the bidirectional coupling that links them. P addresses this by quantifying the full loop’s shared information against a principled upper bound, providing a common scale that is independent of task, reward function, or agent architecture.

Conversely, coupling can remain intact while task difficulty increases, causing reward to drop while P stays stable. This separation matters operationally: coupling failures warrant intervention, whereas increased task difficulty may justify continued operation. The ability to distinguish these regimes is unique to interaction-level monitoring and unavailable to any outcome-based signal.

C. Multi-Channel Detection Succeeds Where Single Signals Fail

The IDT’s detection advantage arises from monitoring multiple projections of the same joint distribution rather than a single quantity. No individual metric dominates: individual coverage ranges from 69–73%, while their union achieves 89.3% — a 16 percentage-point gain with approximately 30 windows lower latency than the best individual channel. Different perturbations disrupt different aspects of the (S, A, S') distribution, making them visible to different channels.

This multi-channel structure addresses a limitation shared by existing information-theoretic approaches. Empowerment [12], [13] quantifies the agent’s capacity to influence future states — a single, unidirectional measure that cannot distinguish whether degradation originates from the environment or the agent. Active Inference [11], [20] monitors prediction error but conflates environmental stochasticity with model misspecification into one signal. Input-drift detectors [7], [8] monitor observations only, missing action-side and coupling-level failures entirely. By decomposing bidirectional coupling into H_f, H_b , and ΔH , the IDT provides directional diagnostic information: H_f -dominated deviations implicate environment-side disruptions, while H_b -dominated deviations implicate agent-side degradation. This directional specificity is unavailable to any single-channel approach and lays the groundwork for automated attribution in future work.

D. Theoretical Foundations and the Agency–Intelligence Distinction

These results instantiate predictions from a first-principles theory that derives bi-predictability from closed-loop information structure and establishes regime-dependent bounds: $P \leq 0.5$ classically, and $P < 0.5$ when agency is present [24]. The observed baseline of $P = 0.33 \pm 0.02$ confirms this prediction, with the gap below 0.5 reflecting the informational cost of action selection — the agent must reserve entropy capacity for choosing among actions, reducing the fraction available for mutual predictability.

This cost connects to foundational results in cybernetics. Ashby’s Law of Requisite Variety requires that a regulator match the variety of its environment [26]; the $P < 0.5$ bound can be read as its information-theoretic expression — coupling efficiency is necessarily traded for action variety. The Conant–Ashby good regulator theorem further requires that effective regulation entails modeling [27]; the IDT provides exactly this

modeling layer, monitoring regulation quality without performing regulation itself.

The theory distinguishes agency from intelligence: agency entails acting on predictions, which trained RL agents satisfy, whereas intelligence additionally requires self-monitoring of P and adaptive regulation. The frozen policies evaluated here exhibit agency but not intelligence. The IDT implements the self-monitoring prerequisite, establishing the signal needed to advance deployed systems from agency toward intelligence.

E. Limitations and Future Work

The full IDT pipeline — P with formal bounds, online computation, and $\pm 3\sigma$ detection — was validated in a single continuous-control environment (HalfCheetah-v4). While the underlying information metrics have shown sensitivity to interaction degradation in robotic manipulation [17], machine vision [25], and language model interactions [24], systematic multi-domain validation of the complete architecture is a key next step.

The estimation pipeline introduces methodological choices that affect sensitivity. Three-bin discretization trades granularity for reliable entropy estimation at available window sizes; finer binning degraded estimates, while quantile-based binning yielded uninformative metrics. The $\pm 3\sigma$ threshold balances false-positive suppression against detection coverage but was not optimized per perturbation type. Window length (300 steps) and stride (50 steps) govern temporal resolution and were selected empirically; their interaction with detection latency in faster or slower dynamical systems remains unexplored.

Finally, the present work validates detection only. Attribution — mapping diagnostic channel responses to specific perturbation types — and reflexive modulation — closing the loop from metric deviation to real-time policy adjustment — are architecturally specified but not experimentally validated. The complementary channel structure suggests the information required for attribution is present in the signal; developing mechanisms to extract and act on it is the immediate next step.

F. From Detection to Self-Regulation

The trajectory from monitoring to self-regulation follows a clear path. This study validates the first layer: real-time detection of coupling degradation from the interaction stream alone. The next layer is attribution — determining whether a detected deviation originates from the environment, the agent’s observations, or its actions. The diagnostic decomposition already provides directional evidence (H_f versus H_b dominance), and systematically mapping these signatures across a richer perturbation space would yield an automated diagnostic capability.

The final layer is reflexive modulation: using sustained deviations in P to adjust the agent’s observation or action interfaces without altering policy weights. The IDT architecture specifies these pathways (Fig. 2, dashed boxes) but does not implement them. Closing this loop would move deployed RL systems from passive agency — acting on learned predictions — toward the self-monitoring and adaptive regulation that the theoretical framework identifies as prerequisites for intelligence [24]. Validating this progression across domains, from

continuous control to manipulation to language, constitutes the broader research program that this work initiates

VIII. CONCLUSION

This paper introduced bi-predictability (P) as a real-time, task-independent measure of RL agent–environment coupling integrity and demonstrated its practical value through the Information Digital Twin architecture. Evaluating SAC and PPO agents on MuJoCo HalfCheetah-v4 across eight perturbation types and 168 trials, we showed three principal results.

First, trained agents exhibit stable coupling at $P = 0.33 \pm 0.02$, below the classical bound of 0.5, confirming the theoretically predicted informational cost of agency. This baseline provides an interpretable, task-independent reference against which coupling degradation can be measured.

Second, IDT-based monitoring detected 89.3% of perturbations compared with 44.0% for reward-based detection, with $4.4 \times$ lower median latency (42 vs. 184 windows; $p < 10^{-6}$). The advantage arises from monitoring coupling structure at the transition level rather than aggregated outcomes — capturing silent degradation that reward signals miss entirely.

Third, the diagnostic decomposition into complementary channels ($P, \Delta H, H_f, H_b$) provides richer detection than any single metric, with the union achieving 16 percentage points higher coverage and approximately 30 windows lower latency than the best individual channel.

These results establish that the information structure of the observation–action–outcome loop carries a deployment-relevant signal invisible to reward-based and single-channel monitoring approaches. Where existing methods track fragments of the interaction — inputs, outputs, or unidirectional influence — bi-predictability monitors the full bidirectional coupling against a principled bound rooted in the same informational constraints that govern any closed-loop regulator. The IDT makes this signal actionable: computable online, without access to internal model parameters or reward functions, and applicable across agent architectures. By providing the detection layer in a progression from monitoring through attribution to reflexive modulation, real-time P monitoring establishes a prerequisite for building RL systems that can detect, diagnose, and ultimately manage their own interaction quality under changing deployment conditions.

REFERENCES

- [1] E. Kaufmann, L. Bauersfeld, A. Loquercio, M. Müller, V. Koltun, and D. Scaramuzza, "Champion-level drone racing using deep reinforcement learning," *Nature*, vol. 620, no. 7976, pp. 982–987, Aug. 2023.
- [2] I. Radosavovic et al., "Real-world humanoid locomotion with reinforcement learning," arXiv preprint arXiv:2303.03381, 2023.
- [3] C. Tang et al., "Legged locomotion in challenging terrains using ego-centric vision," *IEEE Robotics and Automation Letters*, 2024.
- [4] R. S. Sutton and A. G. Barto, *Reinforcement Learning: An Introduction*, 2nd ed. Cambridge, MA, USA: MIT Press, 2018.
- [5] G. Dulac-Arnold et al., "Challenges of real-world reinforcement learning: Definitions, benchmarks and analysis," *Machine Learning*, vol. 110, pp. 2419–2468, 2021.
- [6] J. Josifovski et al., "Continual learning for robotics: A review," *Robotics and Autonomous Systems*, 2024.
- [7] P. W. Koh et al., "Wilds: A benchmark of in-the-wild distribution shifts," in *Proc. Int. Conf. Mach. Learn. (ICML)*, 2021, pp. 5637–5664.
- [8] S. Liang, Y. Li, and R. Srikant, "Enhancing the reliability of out-of-distribution image detection in neural networks," in *Proc. Int. Conf. Learn. Representations (ICLR)*, 2018.
- [9] S. Greco, B. Vacchetti, D. Apiletti, and T. Cerquitelli. "Unsupervised concept drift detection from deep learning representations in real-time." *IEEE Transactions on Knowledge and Data Engineering* (2025)
- [10] S. Levine, A. Kumar, G. Tucker, and J. Fu. "Offline reinforcement learning: Tutorial, review, and perspectives on open problems." *arXiv preprint arXiv:2005.01643* (2020).
- [11] K. Friston, "The free-energy principle: A rough guide to the brain?," *Trends in Cognitive Sciences*, vol. 13, no. 7, pp. 293–301, 2009. (Note: Standard citation for Friston's core Active Inference work).
- [12] K. Friston, T. FitzGerald, F. Rigoli, P. Schwartenbeck, and G. Pezzulo. "Active inference: a process theory." *Neural computation* 29, no. 1 (2017): 1-49.
- [13] A. S. Klyubin, D. Polani, and C. L. Nehaniv, "Empowerment: A universal agent-centric measure of control," in *Proc. IEEE Congr. Evol. Comput.*, 2005, vol. 1, pp. 128–135.
- [14] C. Salge, C. Glackin, and D. Polani, "Empowerment – An introduction," in *Guided Self-Organization: Inception*, Springer, 2014, pp. 67–114.
- [15] M. Grieves and J. Vickers, "Digital twin: Mitigating unpredictable, undesirable emergent behavior in complex systems," in *Transdisciplinary Perspectives on Complex Systems*, Springer, 2017, pp. 85–113.
- [16] F. Tao, M. Zhang, and A. Y. C. Nee, *Digital Twin Driven Smart Manufacturing*. Academic Press, 2019.
- [17] C. Reid, W. Hafez, and A. Nazeri. "Mutual Information Tracks Policy Coherence in Reinforcement Learning." *arXiv preprint arXiv:2509.10423* (2025).
- [18] C. E. Shannon, "A mathematical theory of communication," *Bell System Technical Journal*, vol. 27, no. 3, pp. 379–423, July 1948.
- [19] T. M. Cover and J. A. Thomas, *Elements of Information Theory*, 2nd ed. Hoboken, NJ, USA: Wiley-Interscience, 2006.
- [20] E. Todorov, T. Erez, and Y. Tassa, "MuJoCo: A physics engine for model-based control," in *Proc. IEEE/RSJ Int. Conf. Intell. Robots Syst.*, 2012, pp. 5026–5033.
- [21] T. Haarnoja, A. Zhou, P. Abbeel, and S. Levine, "Soft actor-critic: Off-policy maximum entropy deep reinforcement learning with a stochastic actor," in *Proc. 35th Int. Conf. Mach. Learn.*, 2018, pp. 1861–1870.
- [22] J. Schulman, F. Wolski, P. Dhariwal, A. Radford, and O. Klimov, "Proximal policy optimization algorithms," arXiv preprint arXiv:1707.06347, 2017.
- [23] A. Raffin et al., "Stable-Baselines3: Reliable reinforcement learning implementations," *Journal of Machine Learning Research*, vol. 22, no. 268, pp. 1–8, 2021.
- [24] W. Hafez, C. Wei, R. Felipe, A. Nazeri, and C. Reid, "A Mathematical Theory of Agency and Intelligence," *arXiv preprint arXiv:2602.22519*, Feb. 2026. [Online]. Available: <https://arxiv.org/abs/2602.22519>.
- [25] A. Nazeri, W. Hafez. "Entropy-Based Non-Invasive Reliability Monitoring of Convolutional Neural Networks." *arXiv preprint arXiv:2508.21715* (2025).
- [26] W. R. Ashby. "An introduction to cybernetics." (1956).
- [27] R. C. Conant, and W. R. Ashby. "Every good regulator of a system must be a model of that system." *International journal of systems science* 1, no. 2 (1970): 89-97.